

# Minimum-Cost Bounded-Skew Clock Routing\*

Jason Cong and Cheng-Kok Koh  
UCLA Computer Science Department

310-206-2775 (tel) 310-825-2273 (fax) {cong,kohck}@cs.ucla.edu

## Abstract

In this paper, we present a new clock routing algorithm which minimizes total wirelength under any given path-length skew bound. The algorithm constructs a bounded-skew tree (BST) in two steps: (i) a bottom-up phase to construct a binary tree of *shortest-distance feasible regions* which represent the loci of possible placements of clock entry points, and (ii) a top-down phase to determine the exact locations of clock entry points. Experimental results show that our clock routing algorithm, named BST/DME, can produce a set of routing solutions with skew and wirelength trade-off.

## 1 Introduction

Clock skew minimization is an important issue in the design of high performance circuits. Over the past few years, a number of clock routing algorithms have been proposed, including the H-tree construction for regular systolic arrays [1], the method of means and medians (MMM) by [10], the recursive geometric matching method by [6], and exact zero skew routing under the Elmore delay model by [17]. Recently, the problem of embedding a given *topology* on a Manhattan plane with zero path-length skew is solved optimally by [2, 7] using the *Deferred-Merge Embedding* (DME) algorithm. The algorithm can be either applied to a given clock topology [2] or combined with a clock topology generation algorithm to achieve zero skew with smaller wirelength [7]. Currently, researches on clock routing are moving along a few directions. Zero-skew planar routing was first proposed by [18] using Max-Min operations and followed up by [12, 13] using single-phase DME algorithm. Other work includes buffer insertion [9, 3], process-variation-tolerant skew minimization [15, 4, 14], and a clock router that accomplished specified pin-to-pin delay [16].

The emphasis of most of the current clock routing algorithms is on achieving zero-skew at the expense of longer wirelength, resulting in high power dissipation. In practice, circuits still operate correctly within a tolerable skew bound. Therefore, in order to reduce clock net power dissipation, we believe that the clock routing algorithm should consider bounded-skew trees (BST) instead of zero-skew trees (ZST). In this paper, we propose an algorithm to construct BST based on the DME approach. Our *BST/DME algorithm* first computes shortest-distance feasible regions (as opposed to the merging segment in the original DME algorithm) for the roots of recursively merged subtrees in a bottom-up fashion, followed by a top-down phase to determine the exact embedding of the clock entry points. Experimental results show that as the skew bound increases, we generally see a decrease in total wirelength.

The rest of the paper is organized as follows: In Section 2, we formulate the minimum-cost bounded-skew clock routing problem. In Section 3, we present the BST/DME algorithm under the path-length delay model. Section 4 shows the experimental results obtained by our DME-BST algorithm. Section 5 concludes the paper.

## 2 Problem Formulation

Assume that we are given a set of  $m$  synchronizing components or sinks  $\mathcal{N} = \{N_1, N_2, \dots, N_m\}$  and their locations, denoted  $l(\mathcal{N}) =$

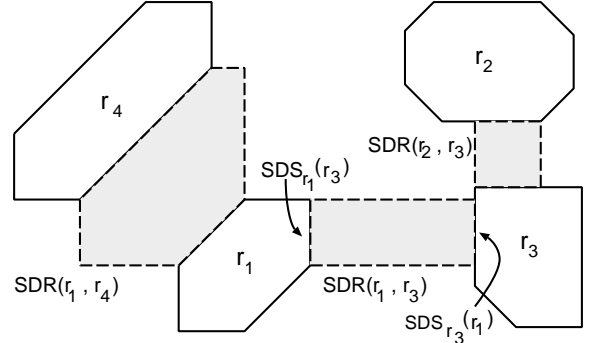


Figure 1: SDRs between regions  $r_1$  and  $r_3$ ,  $r_1$  and  $r_4$ , and  $r_2$  and  $r_3$ .

$\{l(N_1), l(N_2), \dots, l(N_m)\}$ , on a Manhattan plane. The location of the clock source  $N_0$  may be given. A *routing topology*,  $R(\mathcal{N})$ , is a rooted binary tree with  $m$  leaves, each corresponding to a sink. Consider any two nodes, say  $u$  and  $v$ , with a common parent node  $w = p(u) = p(v)$ , then  $w$  corresponds to the *clock entry point* that the clock signal from the source has to pass through before reaching  $u$  and  $v$  (and their descendants).

A clock tree  $T(R(\mathcal{N}))$  is an embedding of the routing topology in the Manhattan plane, i.e. it maps each internal node  $v \in R(\mathcal{N})$  to a location, denoted  $l(v)$ , on the Manhattan plane. Since each node has a unique parent, we denote the edge from any node, say  $u$  to its parent  $w$  uniquely by  $e_u$ . The cost of edge  $e_u$  is its wirelength, denoted  $|e_u|$ . Note that  $|e_u|$  is at least as large as the Manhattan distance between  $l(u)$  and  $l(p(u))$ . The cost of the tree  $T(R(\mathcal{N}))$  is the total wirelength of the edges in  $T(R(\mathcal{N}))$ .

Given a routing tree  $T(R(\mathcal{N}))$ , let  $P(u, v)$  denote the unique path from  $u$  to  $v$  where  $u$  is an ancestor of  $v$  in  $R(\mathcal{N})$ . For a node  $v$  in  $T(R(\mathcal{N}))$ , we use  $T(v)$  to denote the subtree rooted at  $v$ . Under the linear delay model, the signal propagation time from  $u$  to  $v$  is the sum of the wirelengths of the edges in the path  $P(u, v)$ , i.e.  $\sum_{e \in P(u, v)} |e|$ . Let  $PL(u, v)$  denote the signal propagation delay time (more precisely, path-length) from  $u$  to  $v$ . The *skew* of  $T(R(\mathcal{N}))$ , denoted  $skew(T(R(\mathcal{N})))$ , is defined to be the maximum value of  $|PL(N_0, N_i) - PL(N_0, N_j)|$  over all  $N_i, N_j \in \mathcal{N}$ . Given the above definitions, we can formally define the *Minimum-Cost Bounded-Skew Clock Routing* problem as follows:

**Minimum-Cost Bounded Skew Clock Routing Problem (MCBS Problem):** Given a set of sinks  $\mathcal{N}$  with locations  $l(\mathcal{N})$  and a skew bound  $B$ , find a routing topology  $R(\mathcal{N})$  such that a bounded skew tree  $T(R(\mathcal{N}))$  can be constructed with minimum total wirelength and  $skew(T(R(\mathcal{N}))) \leq B$ .

## 3 The BST/DME Algorithm

Our BST/DME algorithm computes a routing tree in two steps. The bottom-up process constructs a tree of *shortest-distance feasible regions* (SDFR) which contain possible locations of the internal nodes in the BST. The top-down process then determines the exact locations of all internal nodes (similar to the DME algorithm). First, we define the following terminology.

\*This work is partially supported by ARPA/CSTO under Contract J-FBI-93-112, the National Science Foundation Young Investigator Award MIP9357582, a grant from Intel Corporation and a Tan Kah Kee Foundation Postgraduate Scholarship.

### 3.1 Definition of SDFR

The *distance* between two points  $u$  and  $v$ , denoted  $d(u, v)$ , is the Manhattan distance between the points. We define the distance between two regions  $r_i$  and  $r_j$ , denoted  $d(r_i, r_j)$ , to be  $\min_{u \in r_i, v \in r_j} d(u, v)$ . The *shortest distance region* (SDR) between two regions  $r_i$  and  $r_j$ , denoted  $SDR(r_i, r_j)$ , is defined to be the set of points  $\{p \mid d(p, r_i) + d(p, r_j) = d(r_i, r_j)\}$ . Figure 1 shows some SDRs between regions. We refer to the segments  $SDS_{r_i}(r_j) = SDR(r_i, r_j) \cap r_i$  and  $SDS_{r_j}(r_i) = SDR(r_i, r_j) \cap r_j$  as the *shortest distance segments* (SDS) that define  $SDR(r_i, r_j)$  (see Figure 1).

Given a routing topology  $R(\mathcal{N})$ , a SDFR of each clock entry point  $v$ , denoted  $SDFR(v)$  is defined recursively as follows:

(i) For each sink  $N_i$ ,  $SDFR(N_i) = \{l(N_i)\}$ .

(ii) For an internal node in  $v_k$  in  $R(\mathcal{N})$  with children  $v_i$  and  $v_j$ ,  $SDFR(v_k)$  is the region of possible placement of  $v_k$  within  $SDR(SDFR(v_i), SDFR(v_j))$  such that the path-length difference from  $v_k$  to any pair of sinks in  $T(v_k)$  is within the skew bound and the *merging cost*  $|e_{v_i}| + |e_{v_j}|$  is minimized.

The above definition is based on the observation that the merging cost of  $v_i$  and  $v_j$  is at least as large as  $d(SDFR(v_i), SDFR(v_j))$ . Therefore, the merging cost is minimized if we can find suitable placement of  $v_k$  in  $SDR(SDFR(v_i), SDFR(v_j))$  such that  $|e_{v_i}| + |e_{v_j}| = d(SDFR(v_i), SDFR(v_j))$ .

Each location  $p$  in a SDFR is associated with two delays (or path-lengths), namely  $SPL(p)$  and  $LPL(p)$  which correspond to the *shortest path-length* and *longest path-length* from  $p$  to the set of sinks rooted under  $p$ , respectively. We define  $skew(p) = LPL(p) - SPL(p)$ . These numbers are used for computing SDFR of its parent node.

### 3.2 Overview of the BST/DME Algorithm

#### Bottom-Up Phase: Topology Construction

Given a set of unconnected sink locations  $l(\mathcal{N})$ , the original topology corresponds to a forest  $\mathcal{F}$  of  $m$  single-node trees. The SDFR of each sink corresponds to its given location, and  $SPL(l(N_i)) = LPL(l(N_i)) = 0$  for  $i = 1 \dots m$ . The bottom-up phase constructs the topology and the tree of SDFRs by repeatedly merging pairs of trees until  $\mathcal{F}$  contains only a single rooted binary tree, which is the routing topology  $R(\mathcal{N})$ . The approach is similar to the clustering-based algorithm in [8].

During each merging step, a *nearest neighbor graph* [8] is constructed. The nodes in the nearest neighbor graph correspond to the roots of trees in the forest. Two nodes  $v_i$  and  $v_j$  are connected in the graph if  $v_j$  is nearest to  $v_i$  or  $v_i$  is nearest to  $v_j$ . The weight of the edge connecting  $v_i$  and  $v_j$  is the distance between  $SDFR(v_i)$  and  $SDFR(v_j)$ . A matching is then obtained by inspecting the first  $s(1, |\mathcal{F}|/k, |\mathcal{F}| - 1)$  edges in the nearest neighbor graph in non-decreasing order, where  $k$  is a parameter  $> 1$  and the function  $s(a, b, c)$ , with  $a \leq c$ , is defined by [8]

$$s(a, b, c) = \begin{cases} a; & a \geq b, \\ b; & a < b < c, \\ c; & b \geq c. \end{cases}$$

For each pair of matched nodes, say  $v_i$  and  $v_j$ , a new clock entry point  $v_k$  which corresponds to the parent node of  $v_i$  and  $v_j$  in the routing topology is introduced. The function  $Merge(SDFR(v_i), SDFR(v_j))$  computes the SDFR of the parent node  $v_k$ . The details of the function is given in the Section 3.4. The outline of the bottom-up phase is given in Figure 2.

#### Top-Down Phase: Topology Embedding

The details of the top-down phase is given in Figure 3. Let  $v_0$  be the root of the routing topology. If the physical location of the clock source  $N_0$  is given, we place  $v_0$  at the nearest location in  $SDFR(v_0)$  from  $l(N_0)$ . Otherwise, we assign  $v_0$  with an arbitrary location (or a location with best skew) in  $SDFR(v_0)$ . We process the rest of the internal nodes of the routing topology in a top-down order. Consider

---

#### Topology Construction Algorithm

---

```

 $\mathcal{F} \leftarrow \emptyset$ 
for each sink  $N_i \in \mathcal{N}$  do
  Create node  $v_i$ 
   $\mathcal{F} \leftarrow \mathcal{F} \cup \{v_i\}$ 
   $SDFR(v_i) \leftarrow l(v_i)$ 
end for
while  $|\mathcal{F}| > 1$  do
  Construct the nearest-neighbor graph  $G$  of  $\mathcal{F}$ 
  For each edge  $(v_i, v_j)$  in the first  $s(1, |\mathcal{F}|/k, |\mathcal{F}| - 1)$ 
  edges of  $G$  in non-decreasing order do
    if  $v_i$  and  $v_j$  are unmatched nodes then
      Mark  $(v_i, v_j)$  as matched
      Create new node  $v_k$ 
       $v_k(\text{children}) \leftarrow \{v_i, v_j\}$ 
      Compute  $SDFR(v_k) \leftarrow Merge(SDFR(v_i), SDFR(v_j))$ 
       $\mathcal{F} \leftarrow \mathcal{F} - \{T(v_i), T(v_j)\} \cup \{T(v_k)\}$ 
    end if
  end for
end while

```

---

Figure 2: The bottom up phase to construct a tree of feasible regions.

---

#### Topology Embedding Algorithm

---

```

 $v_0 \leftarrow \text{root of } R(\mathcal{N})$ 
if  $l(N_0)$  is given then
  Choose  $q \in SDFR(v_0)$  such that
   $d(l(N_0), q) = \min_{p \in SDFR(v_0)} d(l(N_0), p)$ 
else
  Choose any  $q \in SDFR(v_0)$ 
end if
 $l(v_0) \leftarrow q$ 
for each internal node  $v_i \neq v_0$  in  $R(\mathcal{N})$  (top-down order) do
  Let  $v_k$  be the parent node of  $v_i$ 
  Choose  $q \in SDFR(v_i)$  s.t.
   $d(l(v_k), q) = \min_{r \in SDFR(v_i)} d(l(v_k), r)$ 
   $l(v_i) \leftarrow q$ 
end for

```

---

Figure 3: The top-down phase to determine the exact locations of clock entry points.

an internal node  $v_i \neq v_0$ . Let  $v_k = p(v_i)$  be the parent of  $v_i$ . Select a point  $q \in SDFR(v_i)$  such that the distance  $d(l(v_k), q)$  is minimized. Note that  $|e_{v_i}|$  may not be equal to  $d(l(v_k), q)$ .

### 3.3 Properties of BST/DME Algorithm

We can show the following results for our BST/DME algorithm. The proofs of these results are omitted due to page limitation. They are available in our technical report [5].

**Non-overlapping Property:** In each iteration, the SDFRs of the roots of the trees are non-overlapping, and only the boundaries of the SDFRs may touch each other.

**Octilinear Property:** Each feasible region is an *octilinear* convex polygon. The boundary of the region is defined by octilinear line segments, i.e. they are either Manhattan arcs (line segments with slope  $\pm 1$  [2]), or horizontal line segments or vertical line segments.

**Path-Length Property:** For any two points  $p$  and  $q$  on the same Manhattan arc on the boundary of a SDFR,  $SPL(p) = SPL(q)$  and  $LPL(p) = LPL(q)$ . However,  $SPLs$  and  $LPLs$  along a horizontal or vertical line segments do not have such equality property. In general, the changes of skew (due to interaction of different  $SPLs$  and  $LPLs$ ) along horizontal or vertical line segments divide the line segment into three contiguous intervals (one or two intervals may be empty): skew decreases, skew remains equal and skew increases. Along each interval, the  $SPLs$  or  $LPLs$  are strictly increasing or strictly decreasing. The difference between the  $SPLs$  (or  $LPLs$ ) between two points on the same interval is equal to the distance between the points. For example, consider  $p$  and  $q$  on the same interval, then  $|LPL(p) - LPL(q)| = d(p, q)$ .

**Optimality Property:** The BST/DME algorithm is optimal for un-

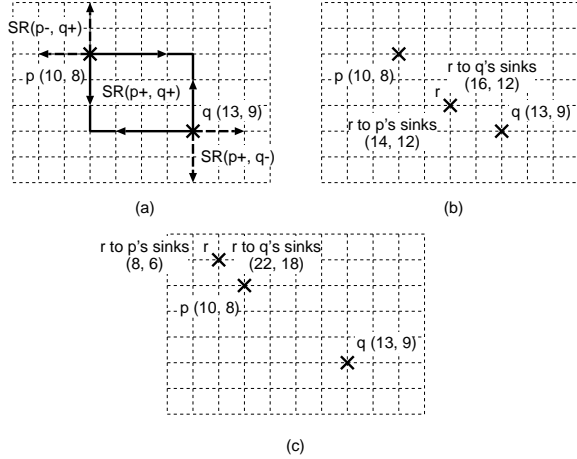


Figure 4: (a) The signed regions defined by  $p$  and  $q$ . (b)  $sd(p, r) = d(p, r)$  and  $sd(q, r) = d(q, r)$ . (c)  $sd(p, r) = -d(p, r)$  and  $sd(q, r) = d(q, r)$ . Each pair of co-ordinates represents ( $LPL, SPL$ ).

bounded path-length skew for a given routing topology.

### 3.4 Merging of SDFRs

Based on the non-overlapping property of the SDFRs at each iteration, the SDR between two SDFRs can be defined by the corresponding pair of SDSs (defined in Section 3.1). Due to the octilinear property of the SDFRs, the pair of SDSs are either a pair of parallel Manhattan arcs, or horizontal line segments or vertical line segments. For simplicity and clarity, we will first illustrate merging of two points. Furthermore, we introduce the notion of *signed distance* between two points.

Consider any two points  $p$  and  $q$ . The pair of points defines three *signed regions*:  $SR(p^+, q^+)$ ,  $SR(p^+, q^-)$  and  $SR(p^-, q^+)$ , collectively referred to as  $SR(p, q)$  (see Figure 4(a)). Now, consider a third point  $r$ . We denote the signed distance of  $r$  from  $p$  and  $q$  by  $sd(p, r)$  and  $sd(q, r)$ , respectively. If  $r$  is in the  $SR(p^+, q^+)$  region, then  $r$  is of positive distance from both  $p$  and  $q$ , i.e.  $sd(p, r) = d(p, r)$  and  $sd(q, r) = d(q, r)$  (Figure 4(b)). If  $r$  is in the  $SR(p^-, q^+)$ , then  $r$  is of negative distance from  $p$  and positive distance from  $q$ , i.e.  $sd(p, r) = -d(p, r)$  and  $sd(q, r) = d(q, r)$  (Figure 4(c)).

Suppose  $r$  is the clock entry point to  $p$  and  $q$ . Then the *signed LPL* (or *SPL*) from  $r$  to any sinks of  $p$  is  $LPL(p) + sd(p, r)$  (or  $SPL(p) + sd(p, r)$ ). We say that signed  $LPL(r)$ , denoted  $SLPL(r)$ , is  $\max(LPL(p) + sd(p, r), LPL(q) + sd(q, r))$  and signed  $SPL(r)$ , denoted  $SSPL(r)$ , is  $\min(SPL(p) + sd(p, r), SPL(q) + sd(q, r))$ . The *feasible region* (FR) of  $r$  under the signed distance metric is defined to be  $FR(r) = \{s \mid s \in SR(p, q), SLPL(s) - SSPL(s) \leq B\}$ . The *core* of the FR, denoted  $CFR(r)$ , is defined to be  $CFR(r) = \{s \mid s \in SR(p, q), SLPL(s) - SSPL(s) = \max(skew(p), skew(q))\}$ .

$FR(r)$  is computed in two steps:

(i) Compute  $CFR(r)$  which is bounded by two line segments within  $SR(p, q)$  such that the two equalities  $sd(p, r) + LPL(p) = sd(q, r) + LPL(q)$  and  $sd(p, r) + SPL(p) = sd(q, r) + SPL(q)$  hold.

(ii) Define  $slack(p, q) = B - \max(skew(p), skew(q))$ . Expand  $CFR(r)$  by  $slack(p, q)/2$  units towards both  $p$  and  $q$ .

For example, Figure 5(a) shows  $CFR(r)$  after merging  $p$  and  $q$ . If  $B = \max(skew(p), skew(q))$ , then  $CFR(r) = FR(r)$ . In Figure 5(b), the skew bound  $B$  is 6 units and  $slack(p, q) = 2$ . We can therefore expand  $CFR(r)$  by one unit towards both  $p$  and  $q$ . It is possible to have part or all of the FR outside of the SDR (Figure 5(c) and (d)).

We shall now present the computation of the FR due to merging

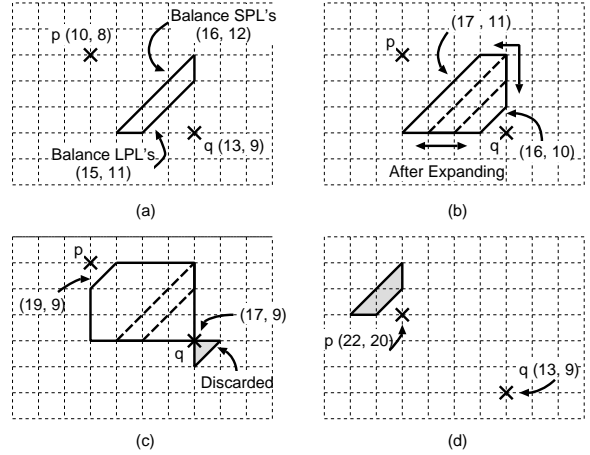


Figure 5: Finding FR of two points  $p$  and  $q$ : (a) Compute  $CFR(r)$  by balancing the  $SPL$ s and  $LPL$ s. (b) Expanding  $CFR(r)$  for a skew bound of 6 units. (c) Expanding  $CFR(r)$  for a skew bound of 10 units. (d) FR between  $p$  and  $q$  for a skew bound of 4 units lies outside of the SDR. Each pair of co-ordinates represents ( $LPL, SPL$ ).

of two SDFRs (or effectively, SDSs). Details are omitted due to page limitation. Since points along a Manhattan arc have the same  $SPL$  and  $LPL$  (path-length property), computation of  $FR$  for a pair of parallel Manhattan arcs is almost identical to that for a pair of points. Therefore, we shall focus on the merging of a pair of horizontal line segments (since merging of vertical line segments is symmetrical to that for horizontal line segments).

Due to the presence of intervals in a line segment (path-length property), we compute the FR (using the 2-step computation) between an end-point of an interval and the point directly opposite it on the other segment for all interval end-points on both segments. For example, Figure 6(a) shows the 5 FRs due to the end-points of the two horizontal line segments. Subsequently, we perform a walk to join the vertices of these FRs to produce the FR of the two horizontal line segments (Figure 6(b)). This is possible due to the path-length property along an interval.

It is possible that the FR may (i) overlap with the SDR (Figure 5(a)–(c) and 6(b)–(c)), or (ii) lie outside of the SDR (Figure 5(d) and 6(d)). In case (i), we take the intersection of the FR and the SDR as the new SDFR. In case (ii), we take the segment of SDSs that is closest to the FR as the new SDFR. For example,  $p$  in Figure 5(d) is chosen to be the SDFR, and the bold horizontal line segment in Figure 6(d) is the new SDFR.

## 4 Experimental Results

We have implemented the BST/DME algorithm in ANSI C for the Sun SPARC station environment. In our experiments, we tested the BST/DME algorithm on benchmark data prim1–prim2 [10] and r1–r5 [17] for  $k$  ranging from 1.5 to 4.0 in the bottom-up phase of the algorithm. Table 1 compares the ZST routing costs by the NN (Nearest Neighbor) algorithm from [7] with the routing costs of our BST/DME algorithm for different skew bounds. The reason that we only compare with [7] is because it outperforms other clock routing algorithms including [2, 6, 17]. Note that the NN algorithm can be improved slightly using the MD and ME algorithms in [7]. Moreover, [8] showed that wirelength can be further reduced by changing the topology after an initial topology is obtained. We are currently incorporating these enhancements in our BST/DME algorithm.

In general, we see a decrease in total wirelengths as the skew increases. However, our results do not compare favorably with [7]

Skew Bound	Circuits						
	prim1 cost / skew	prim2 cost / skew	r1 cost / skew	r2 cost / skew	r3 cost / skew	r4 cost / skew	r5 cost / skew
0 ([7])	131210/0	312430/0	1331867/0	2590670/0	3317598/0	6779690/0	9889688/0
0 (BST/DME)	129105/0	311350/0	1288715/0	2556887/0	3316250/0	6714451/0	9874719/0
100	125480/100	301380/100	1287908/100	2547415/100	3308659/100	6648148/100	9857184/100
200	123695/200	292550/200	1279592/200	2526300/200	3289013/200	6619472/200	9808148/200
500	117905/500	276970/500	1267831/500	2513952/500	3232975/500	6536240/500	9649783/500
1000	112185/1000	267020/1000	1264303/1000	2483180/1000	3213398/1000	6395835/1000	9498362/1000
2000	108225/2000	256380/2000	1242024/2000	2430848/2000	3143449/2000	6267746/2000	9307250/2000
5000	106990/4920	253350/5000	1186527/5000	2337273/5000	2963036/5000	5972735/5000	8801182/5000
$\infty$	105960/8050	249240/9980	1069802/61449	2096325/100260	2710362/122391	5382237/196276	8022978/162786

Table 1: Total wirelengths and skews of the clock routings generated by the BST/DME algorithm for benchmark circuits prim1-2 [10] and r1-5 [17].

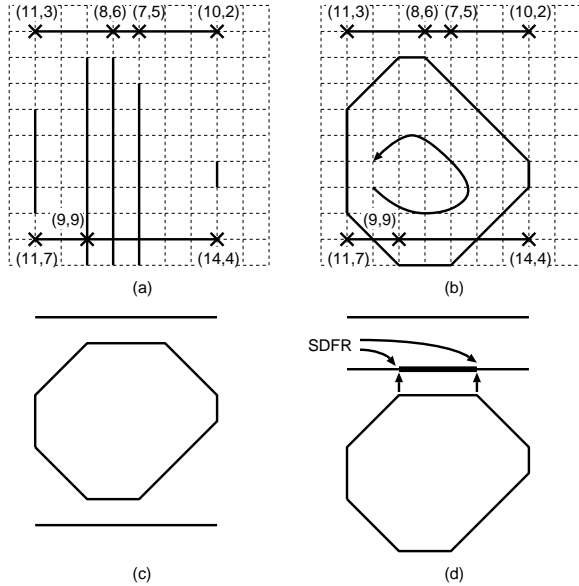


Figure 6: Finding FR of two horizontal line segments: (a) FR of all interval end-points. (b) A walk to produce the resultant FR. (c) FR strictly within the SDR. (d) FR lies outside of the SDR. Note that each pair of co-ordinates represents  $(LPL, SPL)$ .

when it comes to large circuits with small skew. We believe this is due to the computation of new SDFRs when the FRs lie outside of the SDRs (case (ii)). It is also due to this limitation that the algorithm is sub-optimal (for a given topology) when this algorithm is used for ZST routing. However, this approach is optimal (for a given topology) for unbounded skew.

## 5 Conclusion and Future Work

This paper presents a generalized DME algorithm, named BST/DME, which constructs BST by a bottom-up phase which creates a tree of SDFRs, followed by a top-down phase which determines the exact location of the clock entry points. Our clock routing algorithm can produce a set of routing solutions with skew and wirelength trade-off. We learned recently that an independent study of the bounded-skew clock routing problem will be reported in [11].

Most of the current clock routing algorithms first compute the clock routing tree topology and then carry out buffer insertion and wire sizing independently. Also, their emphasis is on achieving zero-skew at the expense of very high power dissipation. Our future plan is to develop a practical clock routing algorithm which carries out simultaneous topology generation, buffer insertion, and wiresizing for achieving bounded skew with minimum power dissipation.

## REFERENCES

- [1] H. Bakoglu, J. T. Walker and J. D. Meindl, "A symmetric clock-distribution tree and optimized high-speed interconnections for reduced clock skew in ULSI and WSI circuits," *Proc. IEEE ICCD*, Port Chester, Oct. 1986, pp. 118–122.
- [2] T.-H. Chao, Y.-C. Hsu, J. M. Ho, K. D. Boese and A. B. Kahng, "Zero skew clock routing with minimum wirelength," *IEEE Trans. on Circuits and Systems*, 39(11), Nov. 1992, pp. 799–814.
- [3] J. D. Cho and M. Sarrafzadeh, "A buffer distribution algorithm for high-speed clock routing," *Proc. ACM/IEEE Design Automation Conf.*, Jun. 1993, pp. 537–543.
- [4] J. Chung and C.-K. Cheng, "Skew sensitivity minimization of buffered clock tree," *Proc. Int'l Conf. on Computer-Aided Design*, 1994, pp. 280–283.
- [5] J. Cong and C.-K. Koh, "Minimum-Cost Bounded-Skew Clock Routing," *UCLA Computer Science Department Technical Report #950003*, January 1995.
- [6] J. Cong, A. B. Kahng and G. Robins, "Matching-based methods for high-performance clock routing," *IEEE Trans. on CAD*, 12(8), August 1993, pp. 1157–1169.
- [7] M. Edahiro, "Minimum path-length equi-distant routing," *IEEE Asia-Pacific Conference on circuits and Systems*, Dec. 1992, pp. 41–46.
- [8] M. Edahiro, "A Clustering-Based Optimization Algorithm in Zero-Skew Routings," *Proc. ACM/IEEE Design Automation Conf.*, Jun. 1993, pp. 612–616.
- [9] L. P. P. van Ginneken, "Buffer placement in distributed RC-tree networks for minimal Elmore delay," *Proc. Int'l Symposium on Circuits and Systems*, 1990, pp. 865–868.
- [10] M. A. B. Jackson, A. Srinivasan and E. S. Kuh, "Clock routing for high performance ICs," *Proc. ACM/IEEE Design Automation Conf.*, 1990, pp. 573–579.
- [11] J. H. Huang, A. B. Kahng and C.-W. A. Tsao, "On the Bounded-Skew Routing Tree Problem", to appear in *Proc. ACM/IEEE Design Automation Conf.*, San Francisco, June 1995.
- [12] A. B. Kahng and C.-W. A. Tsao, "Planar-DME: Improved planar zero-skew clock routing with minimum pathlength delay," *Proc. European Design Automation Conference*, 1994.
- [13] A. B. Kahng and C.-W. A. Tsao, "Low-cost single-layer clock trees with exact zero Elmore delay skew," *Proc. IEEE Int'l Conf. on Computer-Aided Design*, 1994, pp. 213–218.
- [14] S. Lin and C. K. Wong, "Process-variation-tolerant clock skew minimization," *Proc. IEEE Int'l Conf. on Computer-Aided Design*, 1994, pp. 284–288.
- [15] S. Pallela, N. Menezes, J. Omar, and L. Pillage, "Skew and delay optimization for reliable buffered clock trees," *Proc. IEEE Int'l Conf. on Computer-Aided Design*, 1993, pp. 556–562.
- [16] M. Seki, K. Inoue, K. Kato, K. Tsurusaki, S. Fukasawa, H. Sasaki, and M. Aizawa, "A Specified Delay Accomplishing Clock Router Using Multiple Layers," *Proc. IEEE Int'l Conference on Computer-Aided Design*, 1994, pp. 289–292.
- [17] R. S. Tsay, "Exact zero skew," *Proc. IEEE Int'l Conference on Computer-Aided Design*, 1991, pp. 336–339.
- [18] Q. Zhu and W. W.-M. Dai, "Perfect-balance planar clock routing with minimal path-length," *IEEE/ACM Int'l Conference on Computer-Aided Design*, 1992, pp. 473–476.